

Chapter 13

Seasonal Variations of Soluble Organic-Fe(III) in Sediment Porewaters as Revealed by Voltammetric Microelectrodes

M. Taillefert¹, T. F. Rozan², B. T. Glazer², J. Herszage³, R. E. Trouwborst²,
and G. W. Luther, III²

¹School of Earth and Atmospheric Sciences, Georgia Institute of Technology,
Atlanta, GA 30332

²College of Marine Studies, University of Delaware, Lewes, DE 19958

³Department of Inorganic, Analytical and Physical Chemistry, University of Buenos Aires,
Buenos Aires, Argentina

The seasonal cycling of iron and sulfur in the sediment from Rehoboth Bay (Delaware) was examined with solid state Hg/Au voltammetric microelectrodes. High resolution vertical profiles of $\Sigma\text{H}_2\text{S}$, Fe(II), and soluble organic-Fe(III) in the porewaters indicate that dissolved sulfide controls the fate of soluble organic-Fe(III). In the spring and in the fall, dissolved sulfide concentrations are negligible, and soluble Fe(III) and Fe(II) are dominant. This may be explained if the reduction of Fe(III) occurs by dissolution of solid Fe(III), then reduction to Fe(II), or if Fe(II) is oxidized anaerobically in the presence of organic ligands. During the summer, intensive sulfate reduction precipitates iron as FeS and pyrite. Because of its high reactivity and mobility, soluble organic-Fe(III) produced in porewaters can be considered a new reactive electron acceptor.

Introduction

Solid and colloidal iron oxides are commonly involved in the remineralization of natural organic matter in sediments. The reactivity of ferric iron has been assessed on the premise that this species is in its precipitated or colloidal form and that the reduction step proceeds at the surface of the particle (1-4). Kinetic studies have shown that the rate of reduction depends on: (i) the reactivity of the Fe(III) phase, an amorphous species being more reactive than a well-crystallized form; and (ii) the strength of the reductant (1-3). Among reductants present in sediments, dissolved inorganic sulfide may reduce Fe(III) (1, 2, 5, 6), with the rate limiting step being apparently the rate of dissolution of the surface ferrous hydroxide (1). However, more readily available soluble Fe(III) could accelerate the remineralization rate of natural organic matter.

The behavior of soluble Fe(III) at a voltammetric electrode has been described previously (7). Experiments with synthetic solutions showed that soluble Fe(III) (i.e. < 50 nm diameter) reacts at a mercury voltammetric electrode at circumneutral pH if it is complexed by an organic ligand. Several organic-Fe(III) complexes can be detected simultaneously, but they have not been identified. Thus, it is not possible to quantify these electroactive species by voltammetry, and their concentrations are reported in current intensities. Experiments performed in seawater (7) showed that these organic-Fe(III) complexes aggregate with time: their molecular weight increases and their reduction potential simultaneously shifts negatively. Thus, generally "fresh" or less aggregated species measured in natural waters are found around -0.3 V (7, 8), while "aged" or more aggregated species are reduced around -0.6 V (7, 9). These reduction potentials may change slightly with pH and ionic strength.

The reactivity of soluble organic-Fe(III) with dissolved sulfide has been studied in the laboratory with an eight day-old solution of Fe(III) complexed by TRIS (7). Upon addition of bisulfide, Fe(III) is reduced to Fe(II) and the signal for Fe(II) increases drastically. This indicates that the reaction is extremely fast, with a half-time of seconds rather than minutes and hours previously reported with ferrihydrite (6), lepidocrocite (6, 10) and goethite (1). In addition, a non-reductive breakdown of "aged" Fe(III) is promoted when adding bisulfide (7). This breakdown could supplement the production of soluble Fe(III) in aquatic systems, usually promoted by proton dissolution (4), by oxidation of organically complexed ferrous iron with solid ferric oxides (11), or by non-reductive dissolution in the presence of organic ligands (11, 12), including siderophores (13). Fe(II) produced reacts simultaneously with bisulfide to form aqueous FeS (14), but FeS precipitates rapidly, and the voltammetric signals for FeS and Fe(II) usually decrease within minutes. Bisulfide is simultaneously oxidized to elemental sulfur by soluble organic-Fe(III) (7).

In a more recent study (9), the behavior of soluble organic-Fe(III) in two low-ionic-strength anoxic sediment cores from the same site was shown to be controlled by the occurrence of dissolved sulfide. Soluble organic-Fe(III) and Fe(II) were dominant in a sediment core collected from a large creek where dissolved sulfide was negligible. The pH in this system was below the first acidity constant of the sulfide species, which favored the formation of pyrite by reaction of dissolved sulfide with $\text{FeS}_{(s)}$ (Wächterhäuser reaction, 15). Pyrite formation by incorporation of S(0) from elemental sulfur (S_8) and polysulfides (S_x^{2-}) into $\text{FeS}_{(s)}$ was dismissed because this reaction, which probably occurs mainly at the sediment-water interface where S_8 and S_x^{2-} are produced by oxidation of H_2S , is slower than the Wächterhäuser reaction. In addition, the more recent proposed pathway involving the loss of Fe(II) by $\text{FeS}_{(s)}$ followed by incorporation of S(0) into another $\text{FeS}_{(s)}$ (16) was also not considered because this pathway was not consistent with the pH profile in this sediment. These data indicated that the production of dissolved sulfide was the rate limiting step in the Fe(III)- H_2S -pyrite system, thus preserving soluble organic-Fe(III). In contrast in another sediment core collected near a saltmarsh, dissolved sulfide produced by sulfate reduction occurred in significant concentration one centimeter below the sediment-water interface (SWI), and soluble organic-Fe(III) was observed only in the top centimeter of the porewaters. At the onset of dissolved sulfide, soluble organic-Fe(III) was reduced to Fe(II), forming $\text{FeS}_{(aq)}$ which further precipitated. The pH was higher in this sediment, indicating that pyritization rates by the Wächterhäuser mechanism were slower, thus favoring the removal of dissolved sulfide by reduction of soluble organic-Fe(III). These data indicated this system could not be considered at steady-state. The fact that sulfate reduction controls pyritization rates has already been suggested in a recent study comparing different sulfidic environments (17), but the role of pH in controlling pyritization rates has not been evidenced in this study.

In this paper, we report seasonal variations showing that the formation and disappearance of soluble organic-Fe(III) is seasonally controlled by dissolved sulfide and the pH.

Experimental Methods

Sediment cores were collected monthly at the same site (i.e., within a 20 m radius) in Rehoboth Bay (Delaware), a shallow inland bay (water depth ~ 1.5 m) characterized by seasonal eutrophication, and brought back to the laboratory for analysis. Within an hour after sampling, high resolution vertical profiles of O_2 , $\Sigma\text{H}_2\text{S}$ ($= \text{H}_2\text{S} + \text{HS}^- + \text{S}^{2-} + \text{S}^0 + \text{S}_x^{2-}$), Mn(II), Fe(II), $\text{FeS}_{(aq)}$, and soluble organic-Fe(III) were acquired by voltammetry with a Au/Hg microelectrode (18-20) coupled to a potentiostat (DLK-100A, Analytical Instrument Systems).

Minimum detection limits for O_2 , ΣH_2S , Mn(II), and Fe(II), were $2 \mu M$, $<0.2 \mu M$, $5 \mu M$, and $10 \mu M$, respectively. Results for $FeS_{(aq)}$ and soluble organic-Fe(III) measurements are reported in current intensities as the electrochemical sensitivity of these species has not ($FeS_{(aq)}$) or cannot (soluble organic-Fe(III)) be determined. For oxygen measurements, a linear-sweep method was used from $-0.05 V$ to $-1.85 V$ at a scan rate of $200 mV/s$. For ΣH_2S , Mn(II), Fe(II), $FeS_{(aq)}$, and soluble organic-Fe(III) measurements, a square-wave method with a pulse amplitude of $24 mV$ and a scan rate of $200 mV/s$ was used from $-0.1 V$ to $-1.85 V$. A conditioning period was set at $-0.1 V$ for $5 s$ when dissolved sulfide was not present and at $-0.9 V$ for $10 s$ when dissolved sulfide was measured in the porewaters. When dissolved sulfide concentrations exceeded $20 \mu M$, the voltammograms were collected anodically from $-1.8 V$ to $-0.1 V$.

Typical triplicate measurements of soluble organic-Fe(III) obtained by cathodic square wave voltammetry $4 mm$ below the SWI in the porewaters of Rehoboth Bay are shown in Figure 1a. These voltammograms show with good reproducibility a peak at $-0.53 V$ for ferric iron species and a peak at $-1.43 V$ for Fe(II). The Figure 1b displays, also with good reproducibility, a strong dissolved sulfide peak at $-0.65 V$ measured by anodic stripping voltammetry $19 mm$ below the SWI.

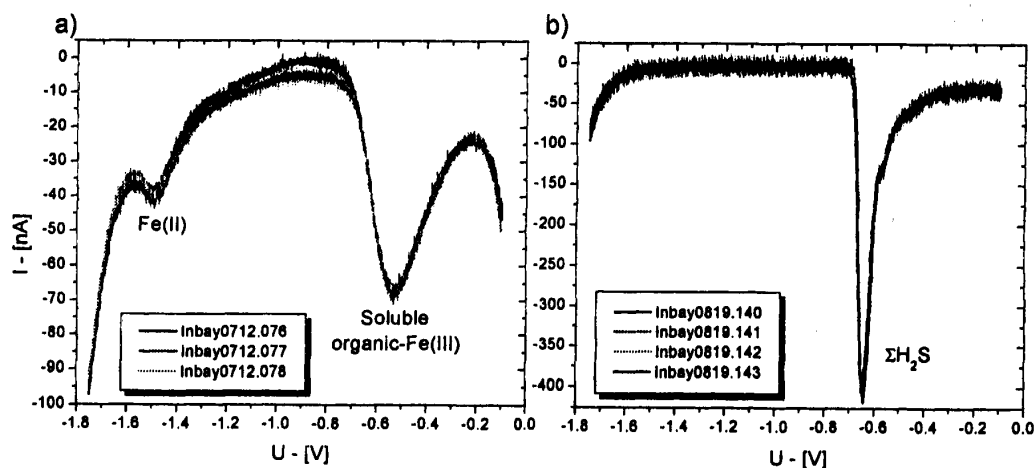


Figure 1. Replicates of square wave voltammograms collected in the sediment porewaters of Rehoboth Bay: a) soluble-organic Fe(III) $4 mm$ below the SWI in July 1999; b) dissolved sulfide $19 mm$ below the SWI in August 1999. The dissolved sulfide profile was measured anodically from -1.8 to $-0.1 V$.

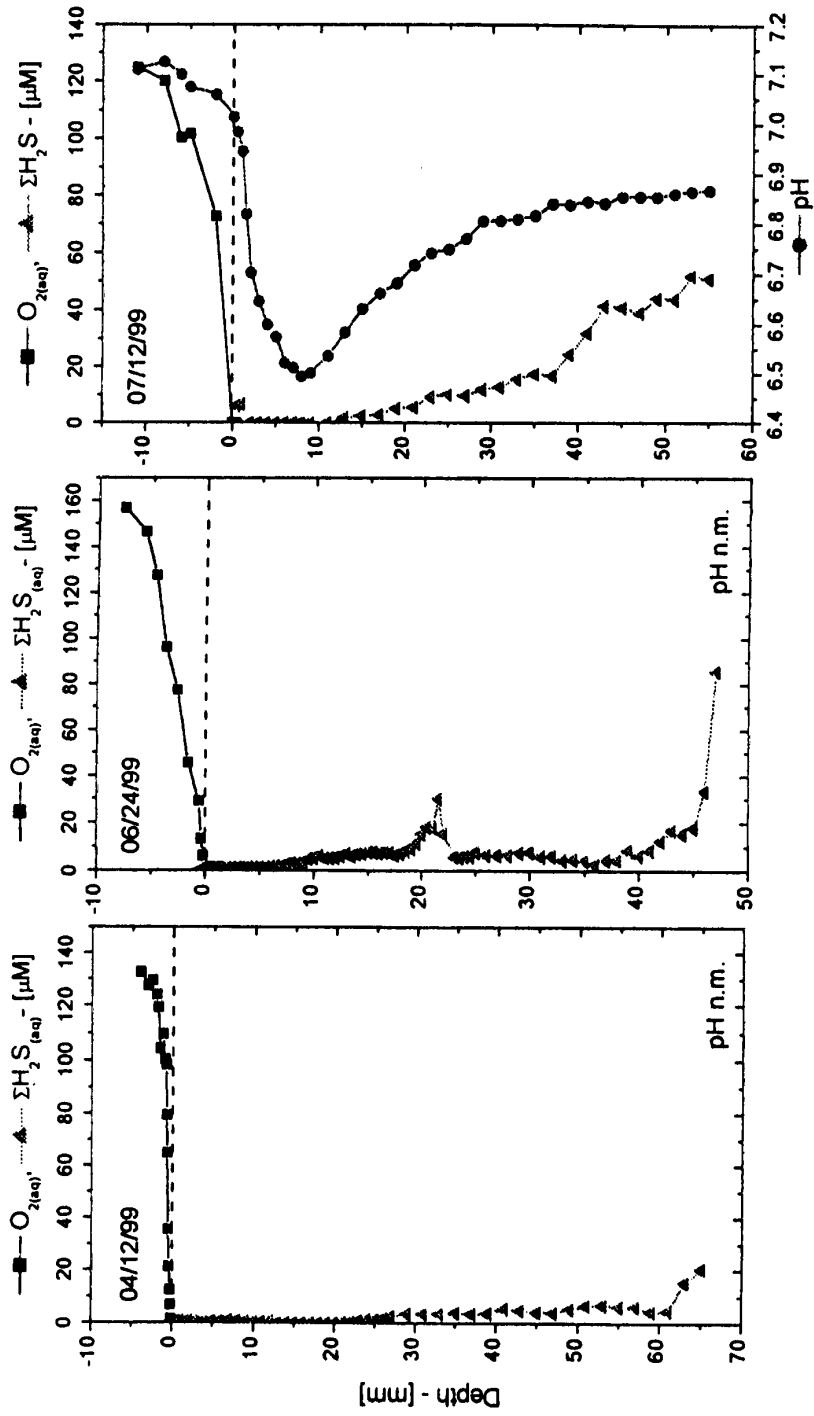
In addition, pH profiles were simultaneously collected from July to October 1999 with a combination pH microelectrode (Diamond General Development Corp.) coupled to a pH-meter (Accumet). The tip of the pH microelectrode was positioned at the same height, but $7 mm$ away from the voltammetric microelectrode, and lowered with a micromanipulator with minimal depth

increments of 0.5 mm. Prior to deployment, the voltammetric microelectrode was calibrated for Mn(II), Fe(II), and $\Sigma\text{H}_2\text{S}$ using the pilot ion method (18). It was also calibrated for oxygen by calculation of its solubility at the temperature and salinity of the overlying waters (21). The pH microelectrode was calibrated by measuring the potential and temperature of buffers at the ionic strength of seawater. The pH in the porewaters was recalculated from the potentials measured and temperature of the overlying waters, assuming the temperature of the core was constant with depth. All the potentials are reported with respect to the Ag/AgCl reference electrode.

Results and Discussion

Electrochemical porewater profiles were collected in April and monthly from June to October 1999. High-resolution vertical profiles of oxygen, dissolved sulfide ($\Sigma\text{H}_2\text{S}$), and pH obtained are displayed in Figure 2. Except for the September data set, oxygen (filled squares) consistently decreases from saturation in the overlying waters a few millimeters above the SWI to insignificant values at the SWI. This indicates that respiration is intense in these sediments during most of the year. The data set of September indicates that oxygen penetrates 2 mm in the sediment, but this core was collected right after the passage of Hurricane Floyd over Rehoboth Bay, suggesting that the surface of the sediment may have been mixed.

The pH is constant around 7 in the overlying waters. Generally, a sharp decrease in pH is observed right below the SWI to a minimum value around the first pK_a of the carbonate system (i.e., 6.28 to 6.5) at a depth varying between 7 and 9 mm. This sharp decrease is followed by a progressive increase in pH deeper in the sediment to ca. 6.9, 6.45, and 6.8 in July, August, and October, respectively. This behavior is observed monthly except in September. After the hurricane, the pH also decreases sharply below the SWI but to ca. 7.2 at a depth of 5 mm only. In addition, this sharp decrease is followed by a constant diminution to a pH of 7.05 at 40 mm. The pH profiles in July, August, and October indicate that remineralization of natural organic matter by oxygen and nitrate occurs within the first 9 mm of the sediment because these reactions release acid equivalents (20, 22). The pH minima indicate the minimum penetration depth of oxygen and/or nitrate and the upper limit of manganese and iron utilization during remineralization (23) since manganese and iron reduction consumes protons (22). Interestingly, the pH rise in August is much smaller than in July and October. This may be explained if the pH is buffered, possibly by the release of protons during precipitation of $\text{FeS}_{(s)}$ (see below).



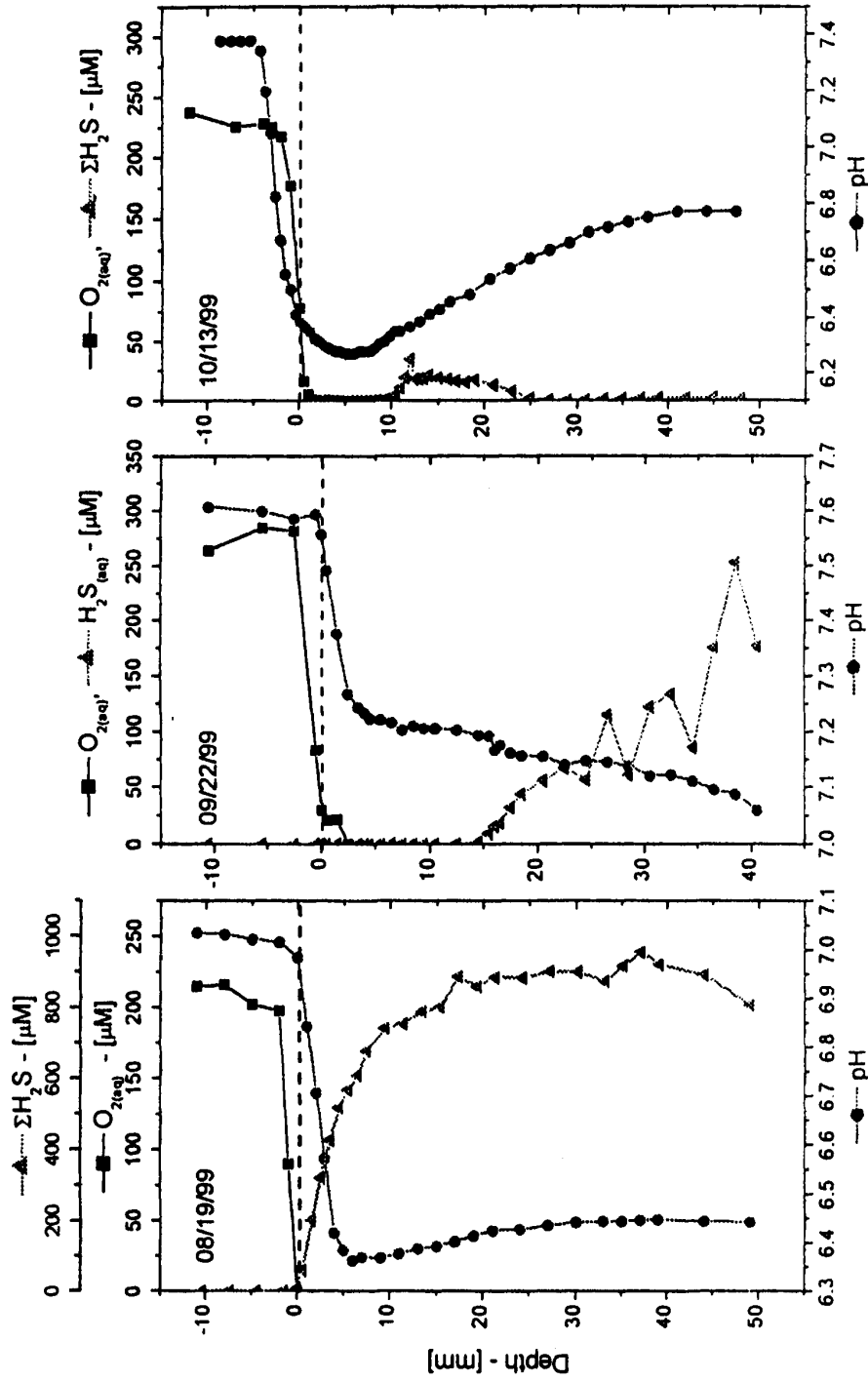


Figure 2. High vertical resolution profiles of O_2 (filled circles), ΣH_2S (filled squares), and pH (filled triangles) in the sediment porewaters of Rehoboth Bay (Delaware) from April to October 1999 (the pH was not measured (n.m.) in May and June). The dashed line represents the SWI.

The fact that the pH measured in September decreases to a depth of 40 mm indicates that the penetration depth of oxygen and nitrate has reached 40 mm, and thus the sediment has been partially mixed during the hurricane, or that the reduction of manganese and iron oxides has been shut down during this event. The pH profile of October shows that the sediment had returned to normal conditions for Rehoboth Bay.

In April, dissolved sulfide is close to the detection limit over the first twenty millimeters and reaches ca. 6 μM between 30 and 60 mm. It is only below 60 mm that the dissolved sulfide concentration increases significantly. In June, the concentration of dissolved sulfide is close to detection limit above 10 mm. It increases regularly below that depth to reach a maximum of 30 μM at 21.5 mm, then decreases to close to detection limit at 35 mm, where $\Sigma\text{H}_2\text{S}$ raises again to 80 μM at 47 mm. In July, small concentrations of dissolved sulfide are measured at the SWI, probably in the form of elemental sulfur (7) or polysulfides (24). Below the SWI, $\Sigma\text{H}_2\text{S}$ stays below detection limit until 10 mm, the depth below which sulfate reduction produces $\Sigma\text{H}_2\text{S}$ to concentrations up to 50 μM at 50 mm. In August, sulfate reduction is extremely intense and dissolved sulfide reaches the SWI with values exceeding 900 μM at depth, the greatest concentrations reached during the studied year. In September, right after Hurricane Floyd, $\Sigma\text{H}_2\text{S}$ is not found until 15 mm below the SWI, but then increases systematically to reach ca. 200 μM at 40 mm. Finally, $\Sigma\text{H}_2\text{S}$ was only detected between 10 and 25 mm in October, with a maximum of 35 μM at 12 mm. A close examination of the sulfide profiles in Figure 2 reveals that the production of dissolved sulfide increases progressively during the spring and early summer and that dissolved sulfide diffuses slowly towards the SWI. In August, the porewaters seem to be saturated with sulfide, and dissolved sulfide probably diffuses to the overlying waters. However, the pH is unusually low for such a high concentration of dissolved sulfide. This may be explained if the system is buffered either by the carbonate system (pH \sim 6.5 close to the pK_a of bicarbonates) or that $\text{FeS}_{(s)}$ precipitation (eq. 1) releases enough acidity to buffer the pH around 6.5:



The profiles of soluble Mn(II), organic-Fe(III), Fe(II), and $\text{FeS}_{(aq)}$ from April to October 1999 are displayed in Figure 3, together with the profiles of O_2 and $\Sigma\text{H}_2\text{S}$ already described in Figure 2. Mn(II) is only above detection limits in July, September and October. This indicates that manganese oxides (MnO_x) are not reduced during remineralization of organic matter in the spring and that Mn(II) has probably fluxed out of the sediment in August.

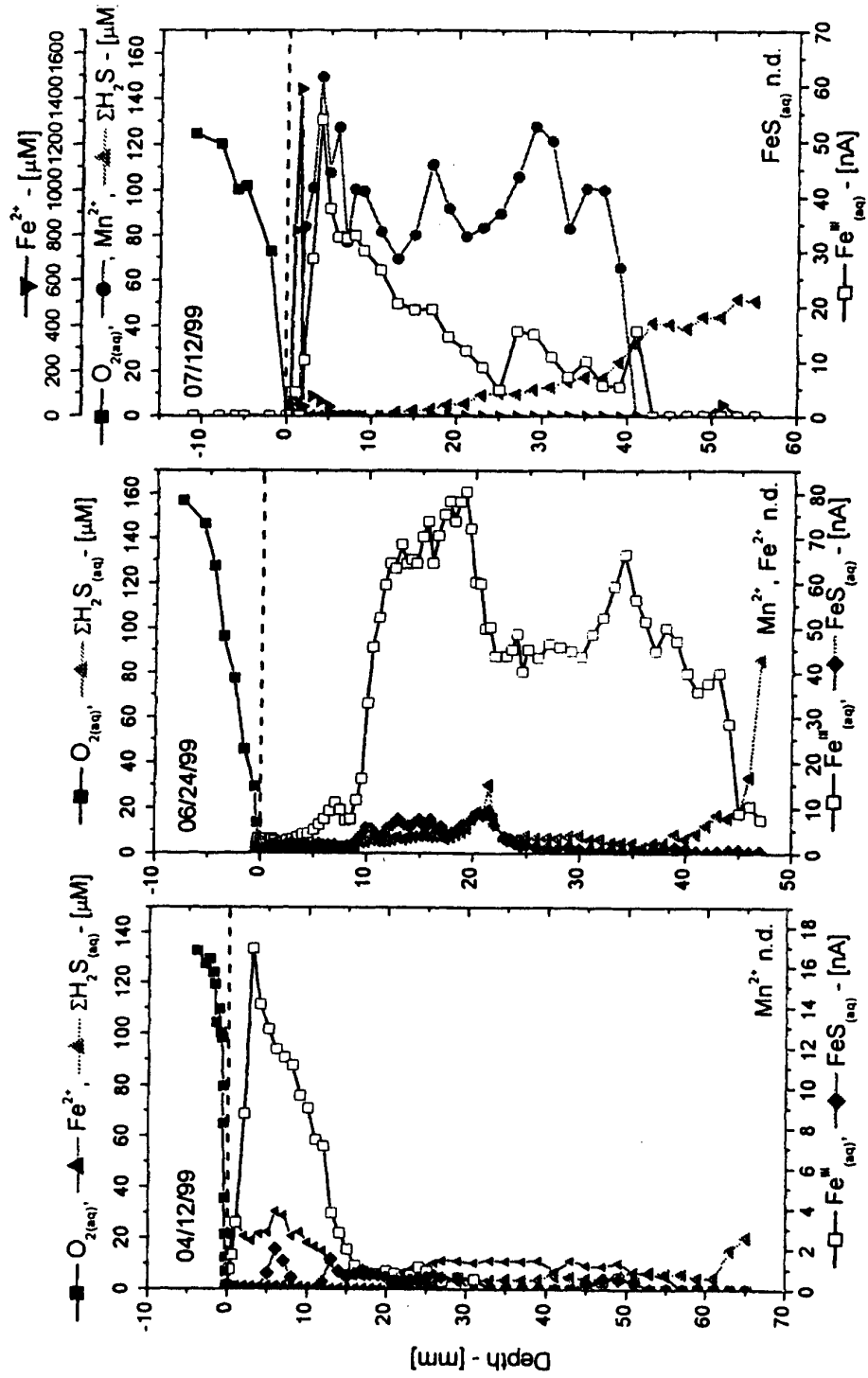
In April, soluble organic-Fe(III) builds up right below the SWI. It reaches a maximum current intensity of 17 nA at 4 mm but decreases to non-detectable values with the onset of dissolved sulfide. Fe(II) and $\text{FeS}_{(\text{aq})}$ are also produced right below the SWI but remain relatively constant and low in the porewaters (ca. 10-30 μM for Fe(II) and 1 nA for $\text{FeS}_{(\text{aq})}$).

In June, soluble organic-Fe(III) is minimal over the first 10 mm. Deeper, it forms a broad peak with a maximum current intensity of 80 nA at 20 mm. Soluble organic-Fe(III) progressively decreases below 20 mm to a minimum of 10 nA, when the concentration of dissolved sulfide increases in the porewaters. Fe(II) and $\text{FeS}_{(\text{aq})}$ are generally low throughout the profile (ca. 10-30 μM for Fe(II) and 5-10 nA for $\text{FeS}_{(\text{aq})}$), but their maximum concentrations coincide with the peak maximum of soluble organic-Fe(III).

In July, Mn(II) is produced 2 mm below the SWI and reaches ca. 150 μM at 4 mm. It decreases slightly to ca. 90 μM between 4 and 7 mm and remains constant to 38 mm. At this depth, Mn(II) decreases in the porewaters to concentrations below the detection limit at 41 mm. Although, dissolved sulfide can reduce manganese oxides with a 1:1 stoichiometric ratio (25, 26), the profiles of Mn(II) and dissolved sulfide show that, assuming a steady-state is reached, manganese oxides are also reduced during remineralization of organic matter and/or Fe(II) oxidation (see below) because the maximum concentration of dissolved sulfide found in July is approximately half of that of Mn(II). A peak of soluble organic-Fe(III) with a maximum current intensity of 55 nA is found 4 mm below the SWI and is coincident with the Mn(II) maximum. In contrast to Mn(II), soluble organic-Fe(III) slowly decreases at the onset of dissolved sulfide to concentrations below the detection limit at 42 mm. Fe(II) forms a very sharp peak with a maximum of ca. 1450 μM 1.5 mm below the interface but decreases to concentrations below detection limit at 6 mm. $\text{FeS}_{(\text{aq})}$ was not detected at this time of the year.

In August, the dissolved sulfide concentration reaches 900 μM and soluble organic-Fe(III) is only detected at the SWI with a small current intensity of 3 nA. In addition, Mn(II) is not detected, and Fe(II) is measured at only one location in the porewaters, while $\text{FeS}_{(\text{aq})}$ forms a peak 5 mm below the SWI with a maximum current intensity of 15 nA.

In September, a peak of Mn(II) is found below the SWI with a concentration reaching 92 μM at 5 mm. At 10 mm, this peak has decreased to ca. 10 μM and remains constant until 25 mm, where Mn(II) is removed from the porewaters. This peak of Mn(II) could result from the input of manganese oxides from the surface during the hurricane followed by rapid reduction. The profiles of Mn(II) and dissolved sulfide in September show that reactive manganese oxides are not present below 25 mm because Mn(II) is not produced with the onset of dissolved sulfide. Soluble organic-Fe(III) is only detected between 26 and 40 mm and remains low as compared to the other months, with current intensities ca. 5 nA.



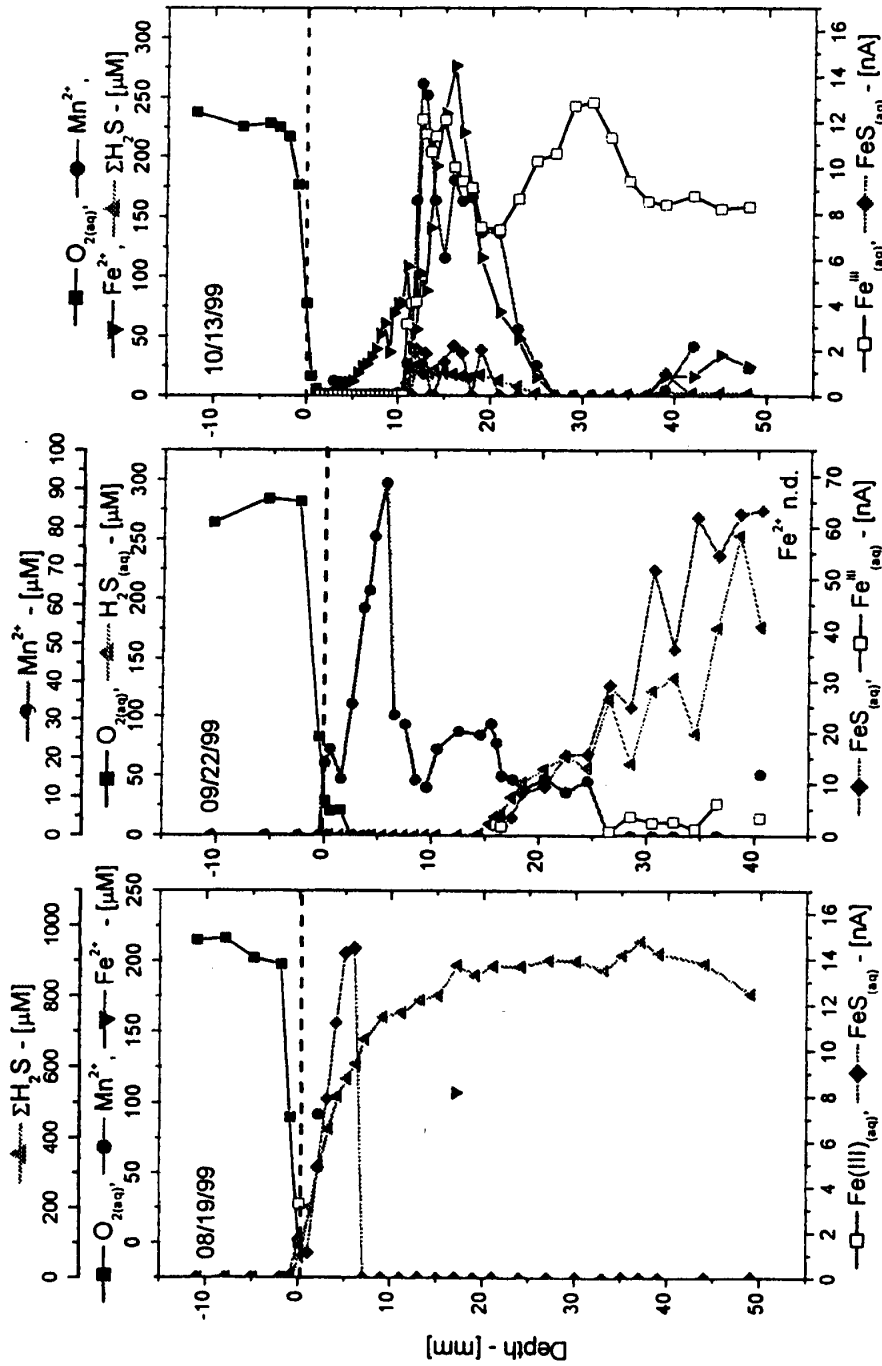


Figure 3. High vertical resolution profiles of soluble organic-Fe(III) (open squares), FeS_(aq) (filled diamonds), Mn(II) (filled circles), Fe(II) (downward triangles), O₂ (filled squares), and ΣH₂S (upward triangles) in the sediment porewaters of Rehoboth Bay from April to October 1999. Species not detected (n.d.) are identified in each profile. The dashed line represents the SWI.

Fe(II) was not detected in the porewaters at this time of the year, but $\text{FeS}_{(\text{aq})}$ increased regularly at the onset of dissolved sulfide to reach a maximum current intensity of 65 nA at the maximum depth of observation.

Finally, in October Mn(II) is observed 3 mm below the SWI and increases with depth to reach a maximum of ca. 280 μM at 16 mm. Its concentration decreases regularly below this maximum to values under detection limit at 28 mm. The peak of Mn(II) and the dissolved sulfide maximum are found at the same location, indicating that Mn(II) could be produced by dissolved sulfide reduction of manganese oxide between 10 and 25 mm. In fact, oxidation of bisulfide by manganese oxides produces elemental sulfur (25, 26), which should be detected as dissolved sulfide by voltammetry (24, 27). These measurements performed after porewater extraction and acidification (not shown) confirmed that dissolved sulfide measured between 10 and 25 mm exclusively consists of elemental sulfur. Soluble organic-Fe(III) is only found below 10 mm, where it increases sharply to reach a maximum current intensity of 12 nA. It remains relatively constant with greater depth because the concentration of dissolved sulfide is low, with current intensities varying between 7 and 13 nA. Fe(II) forms a peak with a maximum concentration of 260 μM between 10 and 26 mm coincident with the peak of Mn(II), $\Sigma\text{H}_2\text{S}$, and soluble organic-Fe(III). It is below detection limit above 10 mm and below 26 mm. $\text{FeS}_{(\text{aq})}$ is low (ca. 1 nA) and only measured where Fe(II) and $\Sigma\text{H}_2\text{S}$ are found simultaneously (i.e., between 10 and 20 mm).

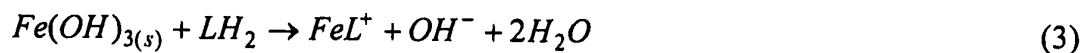
The mechanism of formation of soluble organic-Fe(III) can be inferred from the chemical profiles in the porewaters. Oxidation of Fe(II) in the presence of oxygen and dissolved organic ligands may well produce soluble organic-Fe(III) (7, 25), but this is unlikely in these sediments because the penetration depth of oxygen does not exceed few millimeters below the SWI (Figure 2). Proton promoted non-reductive dissolution is also known to occur but generally below a pH of 6 (4). Manganese oxides may also oxidize Fe(II) (29) and form soluble Fe(III) in the presence of dissolved organic ligands at depth in the sediment. This mechanism, which produces Mn(II), may be significant in July and October at locations where the profiles of soluble organic-Fe(III) and Mn(II) coincide (i.e., between 2 and 40 mm in July and between 10 and 20 mm in October). However, the presence of soluble organic-Fe(III) in May and June as well as below 20 mm in October, when Mn(II) is not observed, indicates that MnO_x reduction is not the sole process producing soluble organic-Fe(III) in these porewaters. Oxidation of Fe(II) by hydrous iron oxides in the presence of organic ligands could be responsible for the formation of soluble organic-Fe(III) complexes. It has been proposed (11, 30, 31) that a Fe(II) complex with a weak-field ligand (i.e., oxygen donor ligand) can facilitate the electron transfer from the Fe(II) to the hydrous iron oxide and thus promote the reductive dissolution of the oxide

and simultaneously produce a soluble Fe(III)-ligand complex (eq. 2). In this equation, one atom of iron is labeled by a star to track its reactive pathway.



The mechanism of electron transfer from the reduced complexed iron to the solid hydrous iron oxide is still open to discussion: on one hand, it is proposed that the weak-field ligand bridges Fe(II) with the hydrous iron oxide through an innersphere complex (30, 31); on the other hand, it is possible that the weak-field ligand is only complexed to Fe(II) and pushes the electron density of Fe(II) directly to Fe(III) without ligand bridging and without formation of a bond between the two iron atoms (11). The latter mechanism involves an outersphere complex and may be faster producing soluble organic-Fe(III). It is important to mention that the rate of oxidation of Fe(II) by hydrous iron oxides in the presence of an organic ligand increases with pH, but the reaction has only been observed in the laboratory below pH ~ 6 (11, 32). Anaerobic oxidation of Fe(II) has been shown to occur biotically in acidic conditions (33, 34) and mediated by nitrate reduction (35). However, the pH is too high in the sediments of the present study to favor such microbial production of soluble organic-Fe(III).

Finally, it has been shown that non-reductive dissolution of amorphous iron oxides by organic ligands can occur at circumneutral pH (4, 11, 36, 37) and that microbial reduction to Fe(II) can be successively faster if solid iron oxides are first non-reductively dissolved in the presence of an organic ligand (12). The composition of the organic ligand promoting the non-reductive dissolution of amorphous iron oxides is not known, but ligands that form mononuclear complexes with iron oxides will facilitate their dissolution (36, 37). In addition, multidentate ligands will further increase the reactivity of iron oxides (38). The proposed reaction (11) is presented in eq. 3 for a mononuclear complex formed with a bidentate ligand.



The porewater profiles of the present study indicate that dissolved sulfide concentrations control the fate of soluble organic-Fe(III). In the spring and the fall, dissolved sulfide concentrations are negligible, and soluble organic-Fe(III) is dominant. During the summer, intensive sulfate reduction produces H₂S which reduces soluble organic-Fe(III) to Fe(II). According to our previous laboratory study (7), the reaction should produce elemental sulfur (eq. 4 in the case of a bidentate ligand).



As a result, soluble organic-Fe(III) always decreases in the porewaters with the onset of dissolved sulfide, and the product of this reaction can form aqueous FeS (eq. 5), which eventually precipitates into solid FeS (eq. 6-1).



Finally, pyrite can be formed by several mechanisms including the Wächterhäuser reaction where FeS reacts rapidly with an excess of dissolved sulfide according to eq. 6-2 and eq. 7 (15, 39):



In July, dissolved sulfide is only produced below one centimeter, and soluble organic-Fe(III) is reduced, but Fe(II) and FeS_(aq) are not observed. In our previous study (9), we showed that the pH was correlated to the amount of FeS_(s) and inversely related to the amount of pyrite found in anoxic sediments. This was explained by the fact that the rate of pyritization by the Wächterhäuser mechanism (eq. 7) increases when the pH decreases below the first acidity constant of dissolved sulfide (pH < 7) because H₂S is the most reactive dissolved sulfide species to form pyrite according to eq. 7 in anoxic conditions. In July, the pH is below 6.8, indicating that, if it occurs, eq. 7 is not the rate limiting step in the formation of pyrite at depth and that pyritization is limited by the supply of Fe(II) and thus FeS_(aq). In August, the excess of dissolved sulfide has completely reduced soluble organic-Fe(III) to Fe(II), and FeS_(aq) is measured within the first centimeter of the porewaters. This indicates that pyritization by the Wächterhäuser reaction is only limited below 8 mm by the production of Fe(II) and FeS_(aq), which depends on the rate of reduction of Fe(III). This is not surprising because the concentration of dissolved sulfide is sufficiently high at this time of the year that pyritization is expected to be limited by the availability of Fe(II). Previous studies, which did not include the reduction of Fe(III) prior to pyritization, have shown that the formations of H₂S and FeS_(aq) are the limiting steps in the formation of pyrite by the Wächterhäuser reaction (15, 39). However, the extreme reactivity of soluble organic-Fe(III) in the presence of dissolved sulfide indicates that the limiting rate in the formation of pyrite can be

the formation of $\text{FeS}_{(\text{aq})}$ (eq. 6-2). In September, the pH reached the highest values found in 1999 in the porewaters (i.e., $7.1 < \text{pH} < 7.5$). This indicates that the rate of pyritization by the Wächterhäuser reaction is relatively slow as this time of the year, which allows $\text{FeS}_{(\text{aq})}$ to accumulate and reach the highest currents measured in 1999 in Rehoboth Bay sediments. Finally, in October the pH decreased to values between 6.3 and 6.8, suggesting that pyritization should be efficient again. However, it has been shown that pyritization can be limited by the rate of sulfate reduction (17). Indeed, the availability of dissolved sulfide in these sediments seems to limit the production of pyrite at this time of the year.

Conclusions

State of the art electrochemical microprofiles were collected from April to October 1999 in the same area in Rehoboth Bay (Delaware). These microprofiles show that electrochemically reactive soluble organic-Fe(III) can be produced in the porewaters as long as dissolved sulfide is not present. This study confirms previous work performed with synthetic solutions (7) that showed soluble organic-Fe(III) complexes are reduced extremely rapidly by dissolved sulfide, as well as other field measurements that demonstrated the incompatibility of reduced sulfur and soluble organic-Fe(III) in sediment porewaters (7, 9).

These new measurements show the seasonal interaction between dissolved sulfide and soluble organic-Fe(III). In the spring, sulfide produced by sulfate reduction is found in low concentrations, suggesting either that sulfate reduction is less intense in the spring season or that sulfide is readily removed from the porewaters. In the summer, sulfate reduction produces millimolar concentrations of dissolved sulfide, preventing the existence of soluble organic-Fe(III) in the porewaters. Finally, in the fall dissolved sulfide concentrations decrease and soluble organic-Fe(III) can build up in the porewaters.

Soluble organic-Fe(III) can be produced by several processes, and its exact source in sediment porewaters remains to be identified. However, three anoxic processes responsible for the production of these complexes in the sediment of Rehoboth Bay can be inferred from the microprofiles obtained by voltammetry. First, oxidation of Fe(II) by reactive manganese oxides followed by complexation by natural organic ligands may partially contribute to the production of soluble organic-Fe(III) in these sediments. Generally, the reduction of reactive manganese oxides with dissolved sulfide is fast, suggesting that competition between soluble organic Fe(III) and manganese oxides may occur in these sediments; Second, the oxidation of Fe(II) by hydrous iron oxides in the presence of organic ligand could be responsible for the formation of soluble organic-Fe(III) complexes. This reaction, usually observed at pH values

very close to those measured in these porewaters, cannot be excluded in these sediments. Finally, the non-reductive dissolution of amorphous iron oxides by organic ligands could also produce soluble organic-Fe(III), which might be an intermediate in the microbial reduction of solid ferric iron to Fe(II).

These measurements seem to indicate that soluble organic-Fe(III) may play an important role in diagenetic processes. Because of its high reactivity and mobility, soluble organic-Fe(III) produced in porewaters may provide an electron acceptor at locations in the sediment where metal oxides are already consumed, potentially shifting the activity of local microbial communities. In addition, the high reactivity of soluble organic-Fe(III) may accelerate the formation of $\text{FeS}_{(\text{aq})}$ and FeS_2 . Finally, these soluble organic-Fe(III) complexes may influence phytoplankton growth in coastal areas. Iron is a very well known limiting nutrient for phytoplankton growth in surface waters, but its source and composition have not been clearly identified. If dissolved sulfide is not produced in the porewaters, soluble organic-Fe(III) may accumulate and eventually diffuse out of the sediment to supply readily bioavailable soluble Fe(III) to the surface waters of coastal marine settings.

Acknowledgements

This research was supported by a NOAA Sea Grant (NA16RG0162-03). We would like to thank two anonymous reviewers for their helpful comments on an earlier version of this paper.

References

1. Pyzik, A. J.; Sommer, S. E. *Geochim. Cosmochim. Acta.* **1981**, *45*, 687-698.
2. Dos Santos Afonso, M.; Stumm, W. *Langmuir.* **1992**, *8*, 1671-1675.
3. Deng, Y.; Stumm, W. *App. Geochem.* **1994**, *9*, 23-36.
4. Zinder, B.; Furrer, G.; Stumm, W. *Geochim. Cosmochim. Acta.* **1986**, *50*, 1861-1869.
5. Canfield, D. E. *Geochim. Cosmochim. Acta.* **1989**, *53*, 619-632.
6. Canfield, D.E.; Raiswell, R.; Bottrell, S. *Am. J. Sci.* **1992**, *292*, 659-683.
7. Taillefert, M.; Bono, A. B.; Luther III, G. W. *Environ. Sci. Technol.* **2000**, *34*, 2169-2177.
8. Rickard, D.; Oldroyd, A.; Cramp, A. *Estuaries.* **1999**, *22(3A)*, 693-701.
9. Taillefert, M.; Hover, V. C.; Rozan, T. F.; Theberge, S. M.; Luther III, G. W. *Estuaries.* **2000**, submitted.
10. Peiffer, S.; Dos Santos Afonso, M.; Wehrli, B.; Gächter, R. *Environ. Sci. Technol.* **1992**, *26*, 2408-2413.

11. Luther III, G. W.; Kostka, J. E.; Church, T. M.; Sulzberger, B.; Stumm, W. *Mar. Chem.* **1992**, *40*, 81-103.
12. Lovley, D. R.; Woodward, J. C. *Chem. Geol.* **1996**, *132*, 19-24.
13. Butler, A. *Science.* **1998**, *281*, 207-210.
14. Theberge, S. M.; Luther III, G. W. *Aquat. Geochem.* **1997**, *3*, 191-211.
15. Rickard, D. *Geochim. Cosmochim. Acta.* **1997**, *61*, 115-134.
16. Wilkin, R. T.; Barnes, H. L. *Geochim. Cosmochim. Acta.* **1996**, *60*, 4167-4179.
17. Hurtgen, M. T.; Lyons, T. W.; Ingall, E. D.; Cruse, A. M. *Am. J. Sci.*, **1999**, *299*, 556-588.
18. Brendel, P. J.; Luther III, G. W. *Environ. Sci. Technol.*, **1995**, *29*, 751-761.
19. Luther III, G. W.; Brendel, P. J.; Lewis, B. L.; Sundby, B.; Lefrançois, L.; Silverberg, N.; Nuzzio, D. B. *Limnol. Oceanogr.* **1998**, *43*(2), 325-333.
20. Luther III, G. W.; Reimers, C. E.; Nuzzio, D. B.; Lovalvo, D. *Environ. Sci. Technol.* **1999**, *33*(23), 4352-4356.
21. Kester, D. R. In *Chemical Oceanography*; Editors: Riley & Skirrow, 1975; 2nd Ed., Volume. 1, Chapter 8, p 498.
22. Froelich, P. N.; Klinkhammer, G. P.; Bender, M. L.; Luedtke, N. A.; Heath, G. R.; Cullen, D.; Dauphin, P. *Geochim. Cosmochim. Acta.* **1979**, *43*, 1075-1090.
23. Van Cappellen, P.; Wang, Y. *Am. J. Sci.* **1996**, *296*, 197-243.
24. Rozan, T. F.; Theberge, S. M.; Luther III, G. W. *Anal. Chim. Acta.* **2000**, *415*, 175-184.
25. Burdige, D. J.; Nealson, K. H. *Geomicrobiol. J.* **1986**, *4*, 361-387.
26. Yao, W.; Millero, F. J. *Geochim. Cosmochim. Acta.* **1993**, *57*, 3359-3365.
27. Wang, F.; Tessier, A.; Buffle, J. *Limnol. Oceanogr.* **1998**, *43*, 1353-1361.
28. Liang, L.; McCarthy, J. F.; Jolley, L. W.; McNabb, J. A.; Melhorn T. L. *Geochim. Cosmochim. Acta.* **1993**, *57*, 1987-1999.
29. Myers, C. R.; Nealson, K. H. *Geochim. Cosmochim. Acta.* **1988**, *52*, 2727-2732.
30. Sulzberger, B.; Suter, D.; Siffert, C.; Banwart, S.; Stumm, W. *Mar. Chem.* **1989**, *28*, 127-144.
31. Stumm, W. *Coll. Surf. A: Physicochem. Eng. Aspects* **1997**, *120*, 143-166.
32. Suter, D.; Banwart, S.; Stumm, W. *Langmuir.* **1991**, *7*, 809-813.
33. Razzell, W.; Trussell, P. C. *J. Bacteriol.* **1963**, *85*, 595-603.
34. Pronk, J. T.; Johnson, D. B. *Geomicrobiol. J.* **1992**, *10*, 153-171.
35. Straub, K. L.; Benz, M.; Shink, B.; Widdel F. *Appl. Environ. Microbiol.* **1996**, *62*, 1458-1460.
36. Bondiotti, G.; Sinniger, J.; Stumm, W. *Coll. Surf.* **1993**, *79*, 157-174.
37. Nowack, B.; Sigg, L. *J. Coll. Interf. Sci.* **1996**, *177*, 106-121.

38. Huheey, J. E.; Keiter, E. A.; Keiter, R. L. 1993. Inorganic chemistry. Principals of structure and reactivity, 4th Ed. HarperCollins College Publishers. New York, NY.
39. Rickard, D.; Luther III, G. W. *Geochim. Cosmochim. Acta.* 1997, 61(1), 135-147.